Fourth LACCEI International Latin American and Caribbean Conference for Engineering and Technology (LACCET'2006)
"Breaking Frontiers and Barriers in Engineering: Education, Research and Practice"
21-23 June 2006, Mayagüez, Puerto Rico.

Flow Assurance in Oil-Gas Pipelines

Mutaz Daas, Ph. D.
Research Scientist, Applied Research Center, Florida International University,
Miami, Florida, USA, mutaz.daas@arc.fiu.edu

Norman Munroe, Ph. D.
Associate Director, Applied Research Center, Florida International University,
Miami, Florida, USA, norman.munroe@arc.fiu.edu

Rajiv Srivastava, Ph. D.
Associate Director, Applied Research Center, Florida International University,
Miami, Florida, USA, rajiv.srivastava@arc.fiu.edu

David Roelant, Ph. D.
Associate Director, Applied Research Center, Florida International University,
Miami, Florida, USA, david.roelant@arc.fiu.edu

Abstract
Pipelines are usually designed to utilize the maximum production rate of an oil field. However, as new oil wells are brought on line in the first few years of an oil field lifetime, production often reaches a peak, then it decreases gradually until it levels off to its economic level. Drag Reducing Agents (DRAs), polymer additives, can be injected into the pipeline to increase its capacity, by decreasing pressure loss, without further mechanical modification or installation of pumping stations at the peak period. Therefore, smaller pipes can be used and significant capital and operating savings can be achieved. The most successful application of DRAs was demonstrated in Trans-Alaska pipeline where not only production rate was increased significantly, but also it was possible to stop construction in two pumping stations along the pipeline.

DRAs are believed to work effectively only in full pipe liquid flow. The paper discusses the applicability and effectiveness of DRA in multiphase pipelines under different scenarios of aggressive flow patters, such as slug flow, and constant variations in pipeline inclinations and fluids rheology. Experimental and computational analysis of the impact of oil-gas mixture rheology, fluids flow rates, and pipe inclination on the effectiveness of DRAs is presented.

Keywords
Oil, Gas, Pipeline, Assurance, Pressure Loss, Slug, Intermittent, Drag Reduction.

1. Introduction

Slug flow is frequently encountered in oil-gas pipelines and is usually accompanied with relatively high-pressure loss more than any other flow pattern. Pressure drop in slug flow can be broken down into three components; frictional, accelerational, and gravitational components. Frictional component of total pressure drop takes place due to the friction between the pipe wall and the liquid in both slug body and liquid film. The pressure drop that results from accelerating the slow moving liquid film ahead of the slug to the slug velocity is called the accelerational component of slug pressure drop. For the flow in inclined pipelines, gravity resists upward flow, and the force spent in driving the fluid upward against the gravity manifests itself as gravitational pressure drop. A schematic of a unit slug is shown in Figure 1.

The current study investigates the influences of oil viscosity and pipe inclination on the contribution of each component to total pressure drop in intermittent slug flow of oil and gas. The performance of the DRA in reducing each component is also investigated. Three kinds of oil of different viscosities, 0.0025 Pa s (density = 800 kg/m^3), 0.026 Pa s (density = 8120 kg/m^3), and 0.05 Pa s (density = 830 kg/m^3), were tested in horizontal as well as near horizontal (2-degree inclination) pipes. Experimental results corresponded well with calculated values.

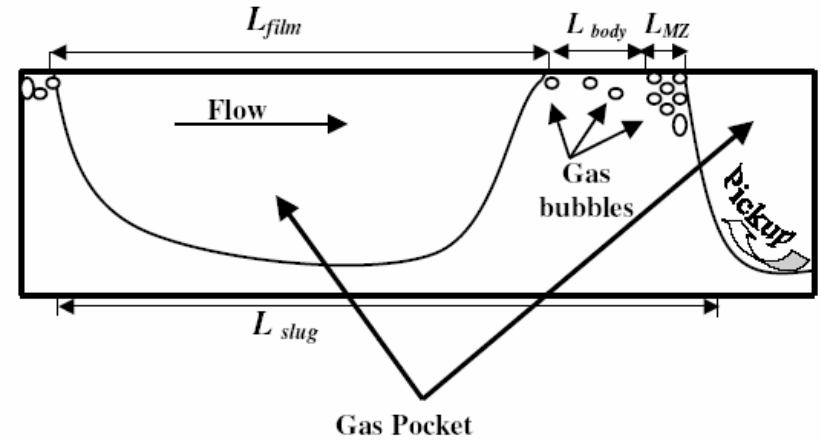

Figure 1: Schematic of a unit slug

2. Experimental Setup

Figure 2 shows the experimental layout of the flow loop used to test the 0.0025 Pa s oil. The experimental work was carried out in horizontal flow loop that was inclinable. This figure shows a 1.2-m^3 stainless steel storage tank that was used as a liquid reservoir. The oil was pumped from the tank using a variable-speed low-shear progressive cavity pump to avoid shear degradation of the DRA. The pump was calibrated before the experiments and a calibration chart was developed and used to measure the flow rate of the liquid phase. The standard deviation of the calibration was within 5%. Carbon dioxide, stored in a 20,000 kg storage tank, was injected into the pipeline at a T-junction where gas and oil are mixed. The gas flow rate was determined by means of a HLIT208 HEADLAND variable area flow meter. The gas then traveled, through a pressure regulator of 0.035-0.862 MPa capacity, into a 40-m long, 5.08-cm ID PVC pipeline before entering the system at the T-junction. The gas flow rate was measured by a variable cross-section in-line pneumatic flow meter (Headland Inc.) before it entered the mixing T-junction. The accuracy of the gas flow meter was within ± 2%. The oil-gas mixture was then allowed to flow through a 20-m long acrylic pipe of 10-cm ID. Two identical SENSOTEC 882-12A 5D differential pressure transducers, with a range of 0 to 0.0345 MPa, and accuracy of ± 0.25% of the readings were used to measure the pressure drop in the test section. This system has been used in similar experimental studies conducted by Daas et al. (2002) . The mixture then returned to the tank where oil and gas were separated. Oil was recycled, whereas gas was vented to the atmosphere. Oil having a viscosity of 0.0025 Pa s and a density of 800 kg/m^3 was used as the liquid phase, whereas carbon dioxide

was the gas phase. Visual measurements were taken by means of a Super VHS Panasonic camera, an AG-190 Panasonic camcorder operating at 60 hertz, an AG 1960 Panasonic VCR, and PVM-1341 Sony TV. The camera was positioned 6 meters back from the upward test section, and the shots were video taped by means of the VCR. The VCR operated at 60 frames/sec and had a digital timer. The camcorder was positioned 2 meters back from the downward test section. The shots coming from the camcorder were recorded directly on VHS tapes. The videos of the flows were played frame by frame to track the flow and capture flow characteristic. The velocity of the liquid film was measured by analyzing closer videos of the test section. Certain bubbles in the liquid film were identified and tracked and the time required to travel certain distance was estimated. Measurements of slug frequency, length and velocity, and the velocity and height of the stratified liquid film ahead of the slug were reported several times at each superficial liquid and gas velocity. The average values were used in the computations. The measurements were within 5% standard deviation.

The drag reducing agent was added to the mixture by preparing a master batch from its required amount based on the total volume of the liquid. The following equation was used to calculate the required volume of DRA for certain concentrations:

$$Q_{DRA} = \frac{C_{DRA} \times Q_{Total}}{1 \times 10^6} \tag{1}$$

where C_{DRA} is the concentration of the drag reducing agent in ppm, Q_{DRA} is the volume of DRA and Q_{Total} is the total volume of liquid. The DRA was then mixed in a 1000-cm^3 beaker with the oil to prepare the master batch. The solubility of DRA in the oil was monitored. This master batch was then poured into the tank through an inlet valve fixed at the top of the tank. The mixture was then circulated in the system for 30 minutes to assure the dissolution of DRA in the liquid phase before beginning the experiments.

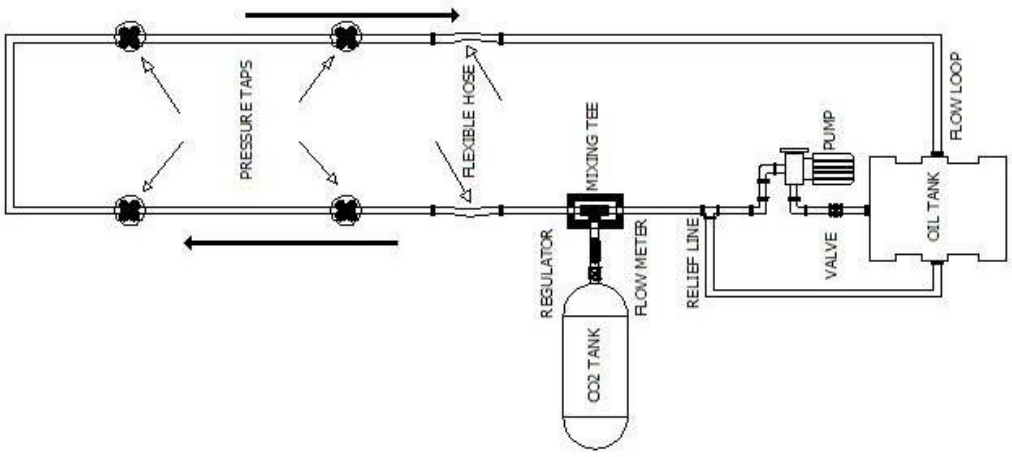

Figure 2: Layout of the inclinable flow loop

The DRA was examined in dosages of 0, 20, and 50 ppm based on a volumetric basis. Superficial liquid velocity had values of 0.5, 1, and 1.5 m/s, while superficial gas velocity varied in the range from 2 to 14 m/s.

A Super VHS Panasonic camera and an AG-190 Panasonic camcorder were positioned 6 and 2 meters back from the upward and downward test sections, respectively. The shots were recorded by high-speed VCR and saved on VHS tapes. The flow was viewed on a TV screen. and flow patterns were reported. Slug frequency, length and velocity were measured. The velocity and height of the stratified liquid film ahead of each slug were measured too.

The experimental layout of the flow loop used to test the 0.05 Pa s oil is shown in Fig. 3. The oil was stored in a 3.5-m^3 cylindrical aluminum storage tank, and two pumps were used during the operation of this system. The oil was pumped using a Moyno low-shear, progressive-cavity, multiphase pump to circulate the oil. This pump was controlled using a Cutler-Hammer IS 905 adjustable frequency drive. An identical pump was used to draw water from the middle of the tank for other experiments that involve water but not considered in this study.

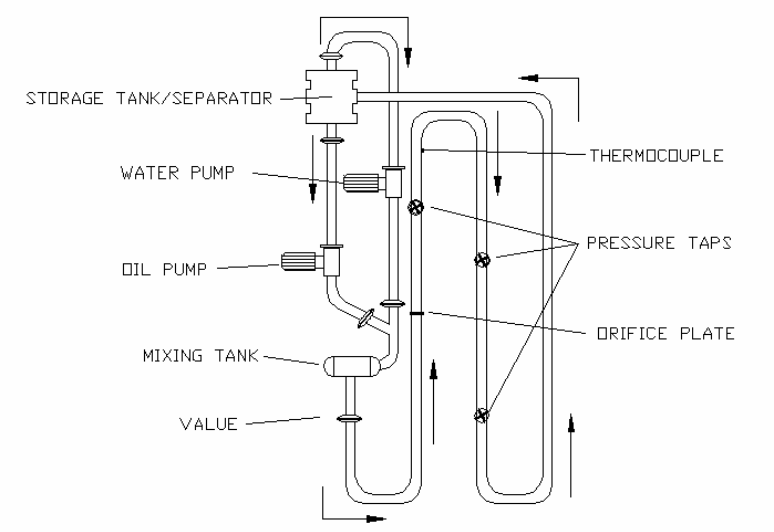

Figure 3: Layout of the horizontal flow loop

The oil was then passed from these pumps into a stainless steel mixing tank where the liquid phase was combined with the gas phase. This mixture then moved into a 10-cm ID, 20-m long acrylic pipeline. Flow characteristics were measured and visually observed in the next 20-m-long acrylic section. Finally, the multiphase mixture of oil and gas was returned to the aluminum storage tank where the gas was vented to the atmosphere and the oil and drag reducing agent was re-circulated. Similarly, the pressure drop was measured in the test section using pressure transducers identical to those used in the 0.0025 Pa s setup.

Carbon dioxide gas was introduced into the system at the top of the mixing tank where it was combined with the liquid and fed from a 20,000-kg storage tank. Gas flow rates were measured using two Omega flow meters placed in parallel. The rates were controlled using a system of ball valves placed in series around the flow meters

3. Computational Methodology

For slug flow, Dukler and Hubbard (1975) produced a model for horizontal systems and defined three parts of the flow. These are the mixing zone, the slug body, and the liquid film behind the slug. A schematic diagram of a stable slug is shown in Fig. 1. This model was used to determine frictional loss in both the slug body and the liquid film behind the slug as well as the accelerational component of total pressure loss that takes place at the front of the slug. Hence, the total pressure drop is estimated using the following equation:

$$\Delta P_T = \Delta P_a + \Delta P_f + \Delta P_g \qquad (2)$$

where ΔP_T is total pressure drop and ΔP_a , ΔP_f , ΔP_g are frictional, accelerational, and gravitational components of total pressure drop respectively.

3.1 Frictional Pressure Loss

Behind the mixing zone in the body of the slug, the pressure drop occurs due to wall friction. For the calculation of this term, the similarity analysis for single-phase frictional pressure drop developed by Dukler *et al.* (1964) is applied. The recommended equation to estimate the frictional pressure loss in the slug body, $\Delta P_{f,\,body}$, is:

$$\Delta P_{f,body} = \frac{2 f_{slug} \left[\rho_G < y_{body} > + \rho_L < 1 - y_{body} >\right] V_{slug}^{\,2} (L_{body} - L_{MZ})}{D} \tag{3}$$

Where V_{slug} is the average velocity of the fluids in the slug body, L_{body} is length of slug body, L_{MZ} is length of mixing zone, y_{body} is gas void fraction within the slug body, and f_{slug} is slug friction factor, which can be calculated using an equation similar to the Blasius equation:

$$f_{slug} = 0.0791 \left(N_{\mathrm{Re}}\right)^{-0.25} \tag{4}$$

Slug Reynolds number, N_{Re}, is defined as:

$$N_{\mathrm{Re}} = D V_{slug} \frac{\rho_G\, y_{body} + \rho_L (1 - y_{body})}{\mu_G\, y_{body} + \mu_L\, (1 - y_{body})} \tag{5}$$

Where D is the pipe diameter. Gregory *et al.* (1978) developed a simple empirical correlation for gas void fraction within the slug body.

$$y_{body} = 1 - \frac{1}{1 + \left[\frac{V_{slug}}{8.66}\right]^{1.39}} \tag{6}$$

Gregory's correlation was developed using data obtained from experimental work in two different pipe sizes (2.58 cm and 5.12 cm I.D.). They utilized light refined oil, with air as the gas phase. The density and viscosity of the oil were 858 kg/m3, and 6.75 mPa sec (0.00675 Pa s) respectively. The range of superficial liquid velocity ranged from 0.03 m/sec to 2.316 m/sec, whereas the superficial gas velocity ranged from 0.088 m/sec to 1.376 m/sec. It is obvious that the correlation would generate quite reasonable estimates for the gas void fraction due to the similarity between the two systems, materials, and flow conditions.

Maley and Jepson (1998) studied the liquid fraction within the mixing zone of the slug. The fluids used were water, and oils with the following viscosities; 0.0025 Pa, 0.0109 Pa s, and 0.0166 Pa s. Nitrogen was used as the gas phase. The pipe diameter was 10 cm (4-inch). They found that the length of mixing zone was independent of liquid viscosity. They proposed the following equation to predict the length of the mixing zone based on the Froude number of the liquid film right behind the slug body, N_{Fr}:

$$L_{MZ} = 0.051 N_{Fr} + 0.18 \tag{7}$$

$$N_{Fr} = \frac{(V_t - V_{film})}{\sqrt{g * H_{film}}} \tag{8}$$

Where V_t is the slug transitional velocity (velocity of the slug front), V_{film} is the average velocity of the liquid film, and H_{film} is the average height of the liquid film behind the slug. A momentum balance on each phase of smooth stratified flow yields the following two equations:

$$-A_G \left(\frac{dP}{dX}\right)_G - \tau_{WG} S_G - \tau_{LG} S_{LG} = 0 \tag{9}$$

$$-A_L \left(\frac{dP}{dX}\right)_L - \tau_{WL} S_L + \tau_{LG} S_{LG} = 0 \tag{10}$$

where $\left(\frac{dP}{dX}\right)$ is the pressure gradient in each phase, τ is shear stress, and S is perimeter. The equation required to estimate τ_{WG}, τ_{WL}, S_G, S_L, S_{LG}, A_G, and A_L were reported by Taitel and Dukler (1976). To simplify the computations, smooth stratified flow was assumed between successive slugs for which $\tau_{LG} \cong \tau_{WG}$. The pressure gradient, $\left(\frac{dP}{dX}\right)$, was calculated by solving equations 9 and 10. The pressure drop across the liquid film can be calculated using the equations below:

$$\Delta P_{f,film} = \left(\frac{dP}{dX}\right)_L * L_{film} \tag{11}$$

$$L_{film} = \frac{V_t}{\theta_{slug}} - L_{body} \tag{12}$$

where L_{film} is the length of the stratified liquid film, L_{body} is the length of slug body, V_t is slug transitional velocity, and θ_{slug} is slug frequency.

3.2 Accelerational Pressure Loss

A slug that has stabilized in length can be considered as a body receiving and losing mass at equal rates. The pressure drop that results from accelerating the slow moving liquid film ahead of a slug to the slug velocity is called the accelerational component of the slug pressure drop, ΔP_a and can be calculated by the following equation (Dukler and Hubbard, 1975):

$$\Delta P_a = \frac{w}{A}(V_{slug} - V_{film}) \tag{13}$$

where w is the rate of mass pickup by the front of the slug, A is the pipe cross section area, and V_{film} is the average velocity of the liquid film. Dukler and Hubbard (1975) proposed the following equation to calculate the rate of mass pickup by the front of the slug, w:

$$w = \rho_L A(1 - y_{film})(V_t - V_{film}) \tag{14}$$

where y_{film} is the gas void fraction in the stratified film. It is evident that the accelerational component is a strong function of the difference between slug transitional velocity, V_t, and the velocity of the liquid film, V_{film}.

In Dukler and Hubbard's model, the holdup in the slug body was assumed to be constant throughout the slug. Again, this is not true at low gas velocities and at liquid velocities near the stratified-slug transition.

3.3 Gravitational Pressure Loss

Fluid density along with pipe inclination played an important role in determining the gravitational component. The gas layer flowing above and parallel to the stratified liquid film was omitted in gravitational computations. The gravitational component was calculated using the following equations:

$$\Delta P_g = \Delta P_{g,body} + \Delta P_{g,film} \tag{15}$$

$$\Delta P_{g,body} \equiv \rho_{slug} \times g \times l_s \times \sin(\theta) \tag{16}$$

$$\Delta P_{g,film} \equiv R_f \times \rho_{oil} \times l_f \times \sin(\theta) \tag{17}$$

The total pressure drop per unit length of the test section; $\frac{\Delta P_T}{\Delta L}$, is estimated by multiplying the pressure drop per unit slug $(\Delta P_T)_{slug}$ by the number of slugs per unit length of the test section at any moment as follows:

$$(\Delta P_T)_{slug} = \left[\left(\Delta P_a + \Delta P_{f,body} + \Delta P_{f,film} + \Delta P_{g,body} + \Delta P_{g,film}\right)\right] \quad (18)$$

$$\left(\frac{\Delta P_T}{\Delta L}\right) = (\Delta P_T)_{slug} \frac{\theta_{slug}}{V_t} \quad (19)$$

where $\frac{\theta_{slug}}{V_t}$ represents the number of slugs per unit length of the test section at any moment.

4. Results and Discussion

Figures 4 through 8 illustrate measured and calculated pressure gradients of the three different oil kinds in horizontal and inclined pipes at superficial liquid velocity of 1 m/s. It is evident that the accelerational component was dominant in the case of low viscosity as shown in Figure 4. The gravitational component of pressure gradient emerged in inclined pipes as shown in Figure 5. Its contribution to total pressure gradient was greater than that of frictional component, yet significantly less than that of the accelerational. Furthermore, the contribution of the accelerational component to total pressure gradient degreased with increasing oil viscosity.

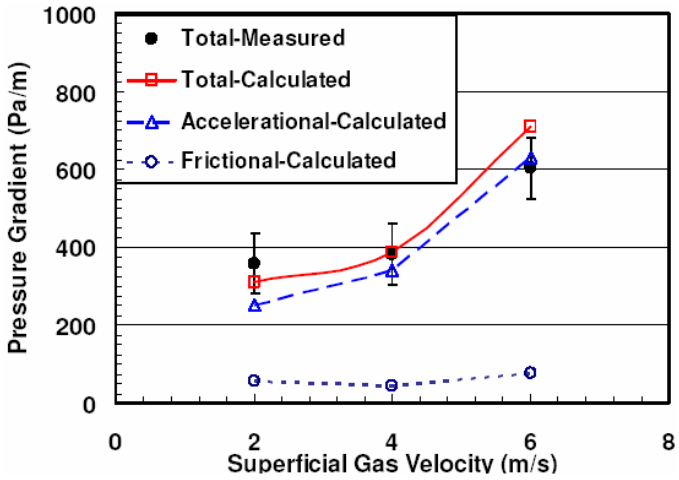

Figure 4: Analysis of pressure gradient for the 2.5 cP oil in horizontal pipes. No DRA

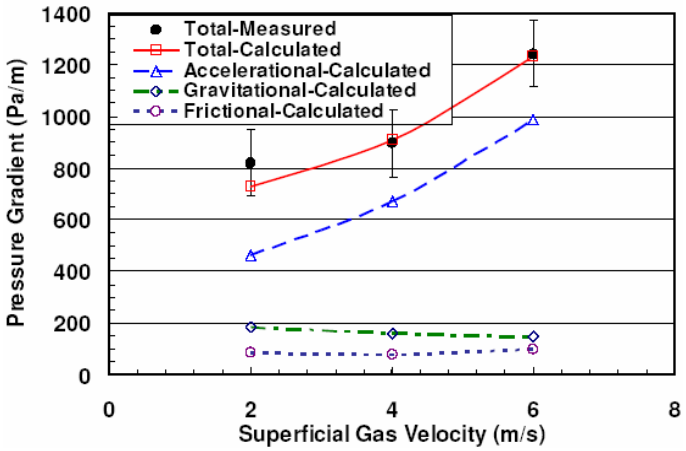

Figure 5: Analysis of pressure gradient for the 26 cP oil in 2-degree upward pipes. No DRA

Figure 6 illustrates a significant increase in pressure gradient when oil viscosity rose from 0.0025 Pa s to 0.05 Pa s in horizontal pipes. Moreover, the magnitude of the difference in pressure gradient as a result of increasing oil viscosity was greater after the addition of DRA. For example, at superficial liquid and gas velocities of 1 m/s and 6 m/s respectively, the pressure gradient increased from 603 Pa/m to 735 Pa/s as a result of increasing oil viscosity from 0.0025 Pa s to 0.05 Pa s. The corresponding increase in pressure gradient after the addition of 50 ppm DRA was from 435 Pa/m to 727 Pa/m. Furthermore, it is clear from Figure 6 that the DRA has higher effectiveness in the case of lower oil viscosity. For example, at superficial liquid and gas velocities of 1 m/s and 4 m/s respectively, the addition of 50 ppm DRA resulted in 51% reduction in pressure gradient of the 0.0025 Pa s oil from 382 Pa/m to 188 Pa/m. The corresponding reduction in the case of 0.05 Pa s was only 9% from 598 Pa/m to 545 Pa/m.

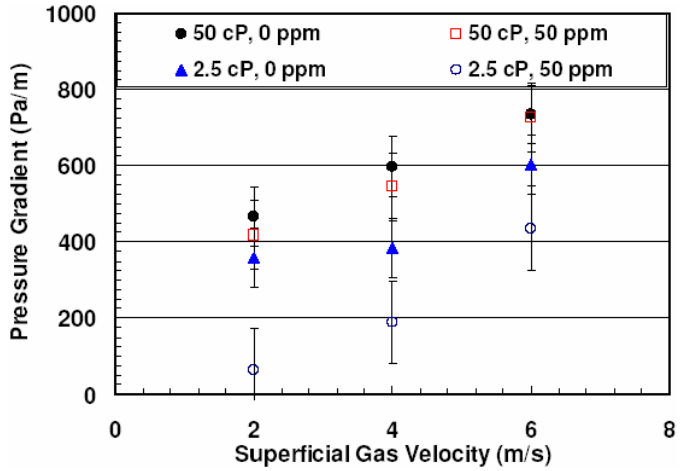

Figure 6: Effects of oil viscosity on total pressure gradient and DRA effectiveness in horizontal pipes

Similar results were noticed in the 2-degree inclined pipes as shown in Figure 7. This figure illustrates the increase in pressure gradient when oil viscosity rose from 0.0025 Pa.s to 0.026 Pa s in upward 2-degree inclined pipes. For instance, at superficial liquid and gas velocities of 1 m/s and 6 m/s respectively, the pressure gradient increased from 912 Pa/m to 1241 Pa/s as a result of increasing oil viscosity from 0.0025 Pa s to 0.026 Pa s. The corresponding increase in pressure gradient after the addition of 50 ppm DRA was from 637 Pa/m to 1113 Pa/m. Moreover, Figure 7 indicates that the DRA has higher effectiveness in the case of lower oil viscosity. For example, at superficial liquid and gas

velocities of 1 m/s and 4 m/s respectively, the addition of 50 ppm DRA resulted in 47% reduction in pressure gradient of the 0.0025 Pa s oil from 649 Pa/m to 342 Pa/m. The corresponding reduction in the case of 0.026 Pa s was only 9% from 896 Pa/m to 813 Pa/m.

Finally, the influence of pipe inclination on both pressure gradient and DRA effectiveness for the case of 0.0025 Pa s oil is shown in Figure 8. It can be seen that significant increase in pressure gradient occurred as a result of slightly increasing pipe inclination from horizontal to 2-degrees upward. Moreover, the magnitude of the difference in pressure gradient as a result of increasing pipe inclination was less after the addition of DRA, unlike the influence of oil viscosity. For example, at superficial liquid and gas velocities of 1 m/s and 6 m/s respectively, the pressure gradient increased from 603 Pa/m to 912 Pa/s as a result of erecting the pipeline 2 degrees upward. The corresponding increase in pressure gradient after the addition of 50 ppm DRA was from 435 Pa/m to 637 Pa/m. Furthermore, it is clear from Figure 8 that the DRA has higher effectiveness in horizontal pipes than in inclined because the gravitational component of pressure gradient is dictated by the fluids densities and pipe inclination. For example, at superficial liquid and gas velocities of 1 m/s, the addition of 50 ppm DRA resulted in 28% reduction in pressure gradient in the horizontal pipes from 603 Pa/m to 435 Pa/m. The corresponding reduction in the 2-degree inclined pipes was 30% from 912 Pa/m to 637 Pa/m.

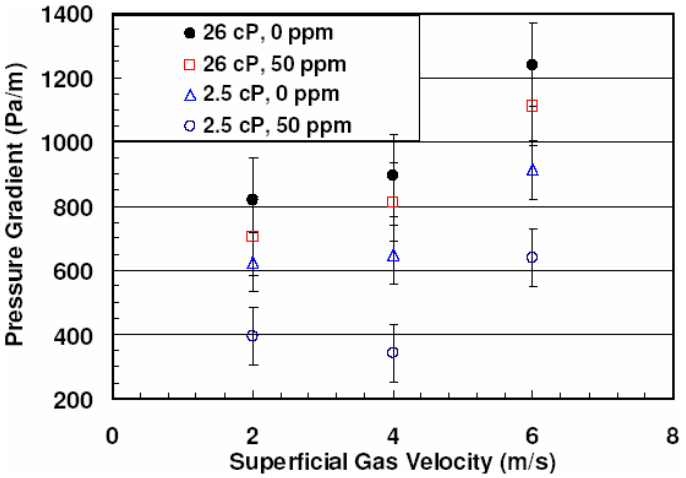

Figure 7: effects of oil viscosity on total pressure gradient and DRA effectiveness in 2-degree inclined pipes

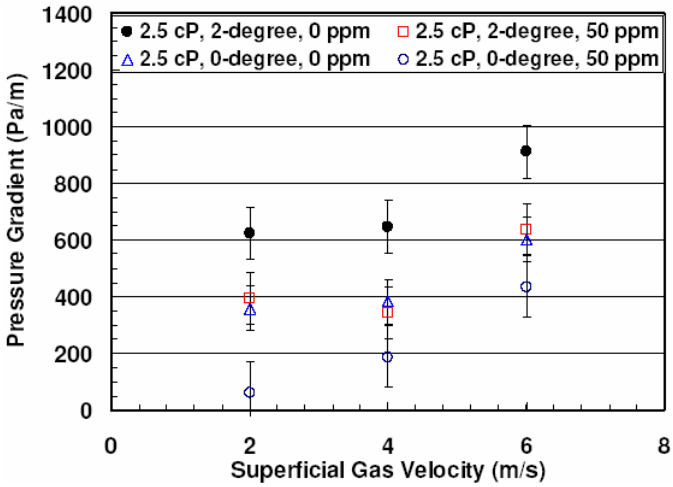

Figure 8: Effects of Pipe inclination on total pressure gradient and DRA effectiveness

5. Conclusions

Experimental investigation and computational analysis were carried out to evaluate the influence of oil viscosity and pipe inclination on both the contribution of each component to total pressure gradient and DRA effectiveness in decreasing pressure loss. The accelerational contribution to total pressure gradient was dominant in the case of low viscosity oil. Frictional contribution increased significantly as oil viscosity increased. A reasonable magnitude of gravitational component emerged when the pipe inclination was increased by 2 degrees.

The effectiveness of utilizing DRA decreased as oil viscosity increased. Moreover, the DRA was more effective in decreasing the pressure gradient in horizontal pipes than in inclined ones.

Acknowledgment

The authors would also like to acknowledge the Center for Corrosion and Multiphase Technology at Ohio University where the experimental work took place.

References

Daas, M., Kang, C., and Jepson, W. P. (2002). "Quantitative Analysis of Drag Reduction in Horizontal Slug Flow". SPE Journal, Vol. 3, pp 337-343.

Dukler, A. E., and Hubbard, M. G. (1975). "A Model for Gas-Liquid Slug Flow in Horizontal and Near Horizontal Tubes". Ind. Chem., Fundam., Vol. 14, pp 337-347.

Dukler, A.E., Wicks, M., and Cleveland, R.G. (1964). "Frictional Pressure Drop in Two-Phase Flow: A Comparison of Existing Correlations for Pressure Loss and Holdup". AIChe J., Vol. 10, pp 38-43.

Gregory, G.A., Nicholas, M.K., and Aziz, K. (1978). "Correlation of Liquid Volume Fraction in the Slug for Horizontal Gas-Liquid Slug Flow". Int. J. Multiphase Flow, Vol. 4, pp 33-39.

Maley, L.C., and Jepson, W.P. (1998). "Liquid Holdup in Large Diameter Horizontal Multiphase Pipelines". Proc. Energy Sources Technology Conference & Exhibition.

Taitel, Y., and Dukler, A. E. (1976). "A Model for Predicting Flow Regime Transitions in Horizontal and Near Horizontal Gas-Liquid Flow". AIChe Journal, Vol. 22, pp 47-55.

Authorization and Disclaimer

Authors authorize LACCEI to publish the papers in the conference proceedings. Neither LACCEI nor the editors are responsible either for the content or for the implications of what is expressed in the paper.